JOURNAL OF MATERIALS SCIENCE 26 (1991) 6207–6217

TEM study of silicon carbide whisker microstructures

S. M. PICKARD*, B. DERBY
Department of Materials, Oxford University, Parks Road, Oxford OX1 3PH, UK
E. A. FEEST
AEA Technology, Harwell Laboratory, Didcot, Oxfordshire OX11 0RA, UK

β-SiC whiskers produced by a number of manufacturers have been examined in the transmission and scanning electron microscopes. In all cases defective microstructures were found with high densities of planar defects such as stacking faults and microtwins. Two distinct types of defective whisker can be identified. The first contains regions of very closely spaced twins on {1 1 1} planes arranged perpendicular to the whisker axis [1 1 1], these were sometimes separated by defect-free regions. In these whiskers a rough surface profile was normal with the roughness closely associated with the highly defective regions of the whisker. The second type of whisker contained stacking faults spaced relatively widely also on {1 1 1} planes but now on the planes inclined to the [1 1 1] axis of the whisker. This leads to a characteristic chevron contrast in the TEM. This second type of whisker had a much smoother surface profile than the first type with perpendicular defects. No whisker contained both defect types but some batches of whiskers contained populations of both types of whisker. The first type of whisker is shown to have defects similar to those reported as common during vapour–liquid–solid whisker growth. This is also consistent with the higher impurity content and the presence of voids found in these whiskers. The second type may be indicative of a different growth mechanism possible under certain conditions of SiC whisker synthesis.

1. Introduction

Whiskers of β-silicon carbide potentially provide effective means of reinforcement for modern metal and ceramic matrix composite materials because of their high strength and stiffness values combined with large aspect ratios. They can be incorporated into metal matrices, usually by melt infiltration or powder metallurgy [1], and have been successful in enhancing the specific stiffness of aluminium alloys [2]. They have also been used as hybridizing additions to enhance the strength of multifilament-reinforced alloys [3]. Their use in ceramic matrices provides highly wear-resistant materials of good thermal shock resistance which have been used as cutting tools [4]. Further exploitation of whisker-reinforced composites will be influenced by the cost, integrity and matrix compatibility of the whiskers used and these factors are, in turn, related to the processes used in their production.

A whisker is usually defined as a single crystal of very high aspect ratio, i.e. ratio of length to diameter, with $L/d \geq 10$ and a diameter in the range $0.01\ \mu m < d < 10\ \mu m$. Such crystal shapes are highly non-equilibrium, with very large surface area to volume ratios. In order for such a structure to be obtained there must be kinetic factors which promote a highly one-dimensional crystal growth. Frank's theory of crystal growth [5, 6] was used by Newkirk and Sears [7] who postulated a screw dislocation down the axis of a whisker which provides a continuous growth step and a preferred growth direction. However, studies of many different whisker types failed to identify axial dislocations, except in one metal [8]. In addition, a dislocation growth mechanism cannot explain many other aspects of whisker morphology nor the nucleation of whisker growth.

The absence of axial dislocations from whiskers implies either a non-dislocation mechanism for growth, or a mechanism of dislocation removal once growth is terminated. Another mechanism for whisker growth from a vapour phase was proposed by Wagner and Ellis [9], the vapour–liquid–solid (VLS) mechanism, for the growth of silicon whiskers. In the VLS mechanism a liquid droplet acts as a receptor of the whisker chemical components from the vapour phase, these then deposit on the growing surface of the whisker from the liquid. The droplet acts as an ideally rough surface for absorption and fast transfer by liquid-phase diffusion can result in rapid whisker growth. Growth in the transverse directions is limited by the size of the VLS droplet. Several whiskers of different elemental or compound composition have been grown by the VLS technique including SiC

* *Present address*: Department of Materials, University of California, Santa Barbara, CA 93106, USA.

0022–2461/91 $03.00 + .12

TABLE I Macroscopic characterizations of whiskers studies

Manufacturer	Approximate year of manufacture	Colour	Range of diameter (μm)	Range of aspect ratios[a]
Tateho	1983	Light brown	0.05–0.5	5–50
Tateho	1988	Light brown	0.05–0.5	5–50
Tokai	1986	Dark green	0.1–1.0	5–50
ARCO[b]	1986	–	0.1–1.5	1–10
Isolite	1988	White	0.1–1.0	> 100

[a] All samples contained small fractions of particulate (aspect ratio = 1) material.
[b] Only available incorporated in a metal matrix composite.

[10, 11]. An extensive review of the VLS mechanism and its applications has been published by Givargizov [12].

Many manufacturing routes for producing SiC whiskers have been described in the technical and patent literature. Most are variants of two main families:

(i) pyrolysis of solid silicon and carbon sources in a non-oxidizing atmosphere;
(ii) pyrolysis of gaseous sources of silicon or silicon and carbon, usually by involving hydrogen as a carrier gas.

Within each family the variants are mainly concerned with ways of increasing yield, uniformity and purity or reducing costs. An example of the former [13] describes the multiple steps from pretreating cereal chaff as the silicon source through to the production and separation out of Si_3N_4 whiskers, the addition of further feedstock for pyrolysis, the separation out of SiC whiskers, the removal of excess carbon and the recovery of SiC powder. An example of the latter [14] involves the introduction of a silicon halide gas, a hydrocarbon gas and hydrogen into a reactor containing an SiC-bearing substrate.

In the case of the pyrolysis of compacts of carbon and either silicon [15] or silicon-containing minerals or cereal chaffs, e.g. rice husks [16, 17], the important reactions are believed to be a carbothermal reduction of the silica to produce CO and SiO gaseous species. Comer [18] proposed the subsequent formation of SiC by a chemical vapour deposition CVD reaction between SiO and CO. The VLS mechanism of SiC growth proposed by Milewski *et al.* [11] has the deposition of silicon and carbon in a liquid metal catalyst from SiO and CO gaseous phases produced in separate gas generators, these then react to form SiC. A similar VLS step has been proposed by Nutt [19] to explain the influence of metallic impurities on whiskers produced by rice husk pyrolysis. A VLS mechanism is also possible in the growth of SiC whiskers by the thermal decomposition of methyltrichlorosilane in hydrogen reported by Merz [20].

In this study, samples of β-SiC whiskers obtained from various manufacturers were examined by transmission electron microscopy. Whiskers from different manufacturers are shown to have characteristically different defect structures. Twins, stacking faults, grain boundaries and microvoids were identified in the whiskers. These are compared with defects reported in SiC whiskers in previous electron microscopy examinations. A recent study [21], has investigated the bulk phase analysis, chemical composition and surface chemistry of a number of different sourced SiC whiskers produced by the pyrolysis route. The present study consists of a more detailed TEM investigation of this range of whisker materials and others.

2. Microstructural observations

The whiskers, in the as-received state, were electron transparent at 200 kV so that the most convenient means for the analysis of loose fibres was to clamp them in a folding grid and examine them directly in the microscope. One whisker sample was of a sufficiently large aspect ratio that it could be clamped in an open grid but it was normal with fine whiskers to use a carbon grid. Whiskers were never handled in the bulk in the open laboratory because of fears about the potential toxicity of such small diameter fibres [22]. Some whiskers were only available in a metal matrix and others were incorporated into such matrices to allow sectioning and the observation of transverse views of the whisker. In these cases mechanical thinning followed by ion-beam etching was used to create electron-transparent regions of the whisker. High-resolution microscopy and lattice imaging was carried out on a Jeol 200CX microscope. Electron probe microanalysis was carried out in a Philips CM12 analytical microscope and in a VG HB501 STEM system which was capable of EELS light element analysis.

Whiskers of two distinct morphologies were studied. Whiskers of comparatively short aspect ratio with some equiaxed particles covering an approximate range of aspect ratios from 5–50 were obtained loose (Tateho and Tokai). When examined loose these whiskers behaved in a similar manner to highly agglomerated ceramic powders. Their colour was a dull green or brown. Whiskers of similar aspect ratio were obtained (ARCO) incorporated in a 2124 aluminium alloy matrix. These three whiskers were assumed to have been manufactured by a similar route, probably pyrolysis of cereal chaffs or similar silica- and carbon-containing systems. One further whisker sample (Isolite) was investigated; this had a strikingly different appearance from the previously mentioned whiskers. These too were supplied loose but were white in colour and came as a fibrous mat, similar in appearance to cotton wool, but made up from ceramic

whiskers 3–5 mm long. These properties of the whiskers are tabulated in Table I along with their probable year of manufacture.

2.1. Isolite whiskers

Fig. 1 shows the Isolite whiskers as long fibres of practically constant diameter in the range 0.1–1 μm with length up to about 5 mm. The fibres were rounded in sections of high aspect ratio with some branching. The larger diameter whiskers generally showed an internal defect structure which under normal bright-field imaging appeared (Fig. 2) as a type of strain contrast with the defects visible running at an angle of 36° to the ⟨1 1 1⟩ whisker axis (and presumed growth direction) when oriented perpendicular to the beam, showing the defects to be on {1 1 1} planes. The defects were often widely separated and were further identified as stacking faults by the stacking-fault fringe contrast observed when the defects were inclined at a steep angle to the beam (Fig. 3). The diffraction pattern taken from these defective whiskers was of β-SiC and showed streaking perpendicular to the defect planes indicating a very narrow defect width. High-resolution images shown in Fig. 4 resolve the defects to a single lattice plane and therefore identify them as intrinsic stacking faults. In the smaller diameter whiskers a second defect type was visible running normal to the whisker axis (Fig. 5). These lamella-like regions were comparatively rare and were usually widely spaced along whiskers where they did occur. It proved impossible to obtain diffraction data from these small regions. Regions between these defects appeared free of further defects and dislocations. These two defect types were never seen in the same whisker and it is thus believed that they may possibly indicate two different growth mechanisms under the conditions of manufacture.

A thin amorphous region was sometimes found surrounding the whiskers (Fig. 6). In some of the

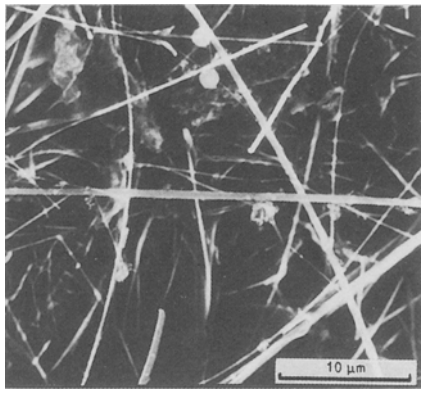

Figure 1 SEM image of the Isolite whiskers showing long, uniform diameter, whiskers.

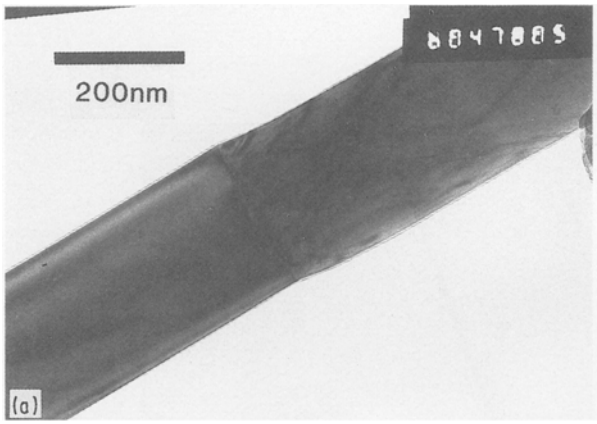

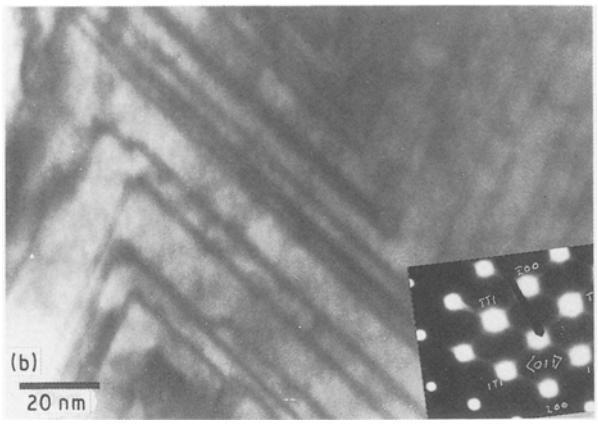

Figure 2 Isolite whiskers. (a) Transmission electron micrograph showing a small-angle grain boundary and the presence of the characteristic chevron defect markings. (b) Higher magnification TEM image of the chevron defects, with inset diffraction pattern showing streaking perpendicular to the defect planes.

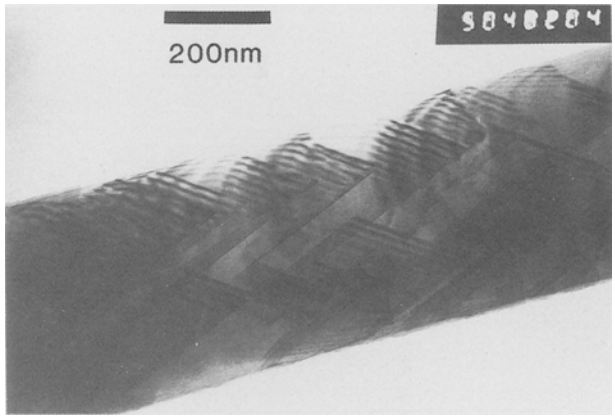

Figure 3 Contrast bands revealed on tilting Isolite whiskers containing the chevron defects indicate the presence of a stacking fault.

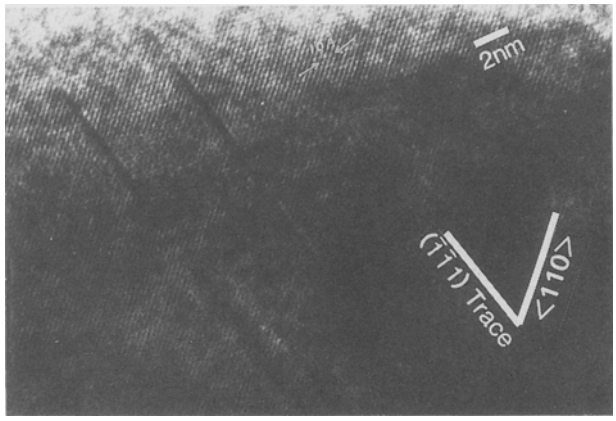

Figure 4 High-resolution transmission electron micrograph of the defects in the chevron region show very narrow stacking faults.

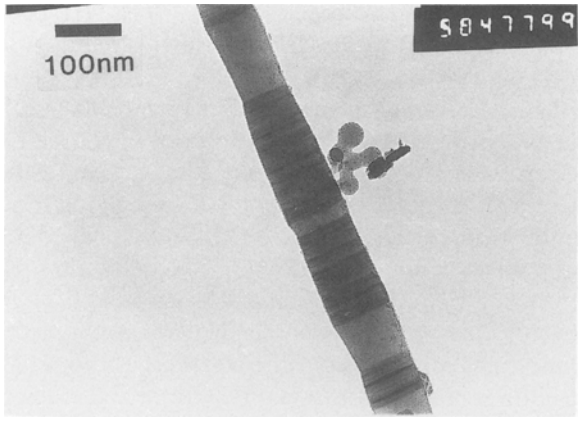

Figure 5 Thinner Isolite whiskers showing defects transverse to the fibre axis spaced by perfect material.

thinner whiskers this seemed to form much thicker bulbous defects (Fig. 7a); on higher magnification SEM imaging the whisker can be seen continuing through one of these bulges (Fig. 7b). Thinner bulges could be imaged in the TEM (Fig. 7c) and here the bulged region was found to be amorphous and possibly nucleated around small regions containing transverse defects. Energy-dispersive X-ray (EDX) microanalysis of the whiskers was carried out in a VG HB501 STEM fitted with windowless detectors for light element and analysis. These are shown in Fig. 8 and indicate a predominance of silicon, carbon and oxygen as the main whisker constituents. Strong copper peaks are generated by the copper grid used to clamp the whiskers for examination. In Fig. 8a the central region of a whisker shows strong silicon and

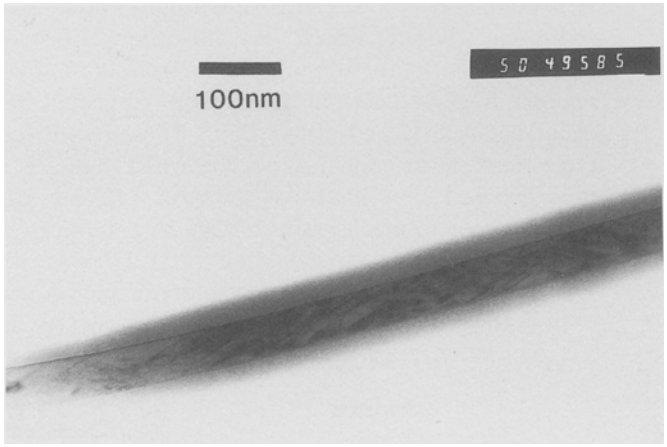

Figure 6 Isolite whisker surrounded by a thin amorphous coating.

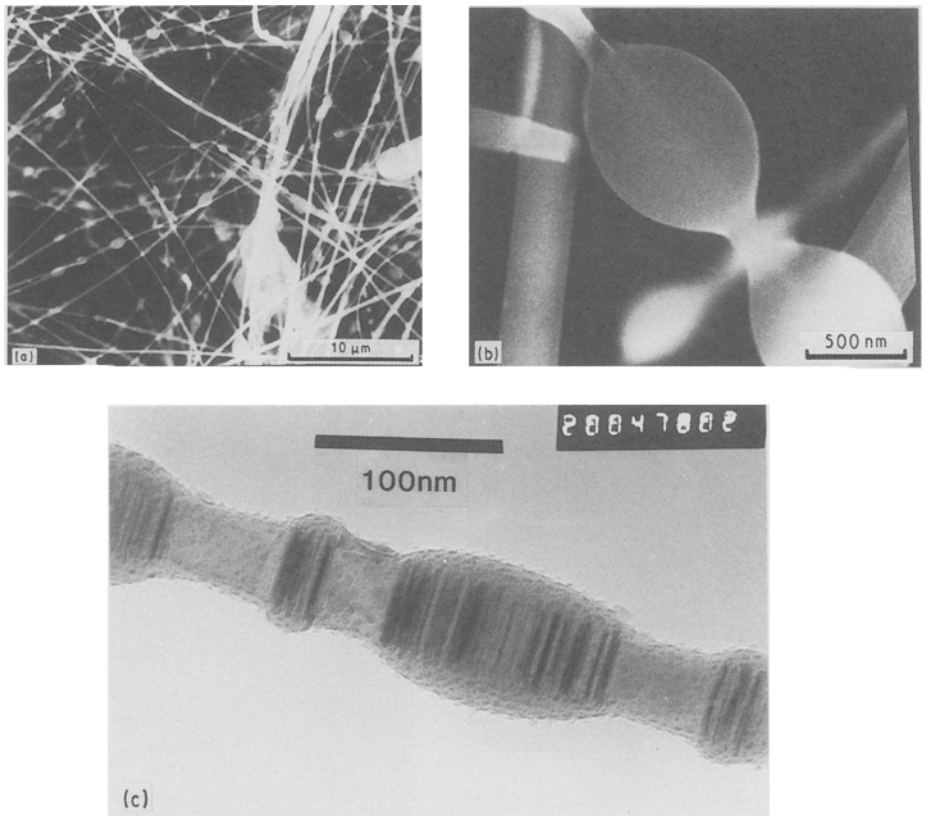

Figure 7 The amorphous coating occasionally formed large bulbous regions on the Isolite whiskers. (a) General SEM view of whiskers, some containing bulges. (b) Higher magnification SEM image of a bulged whisker. A whisker can be seen to continue through the bulges. (c) TEM imaging shows that a thickening of the coating is associated with transverse defects in some whiskers.

carbon peaks and a weak oxygen peak, microanalysis near the edge of a whisker (Fig. 8b) shows a much stronger oxygen peak suggesting that the amorphous surface region is predominantly SiO_2 in composition. In Fig. 8c an isolated spherical inclusion is analysed showing no carbon peak, it is almost certainly amorphous SiO_2 but contains calcium and sulphur impurities not detected in whiskers. The isolite

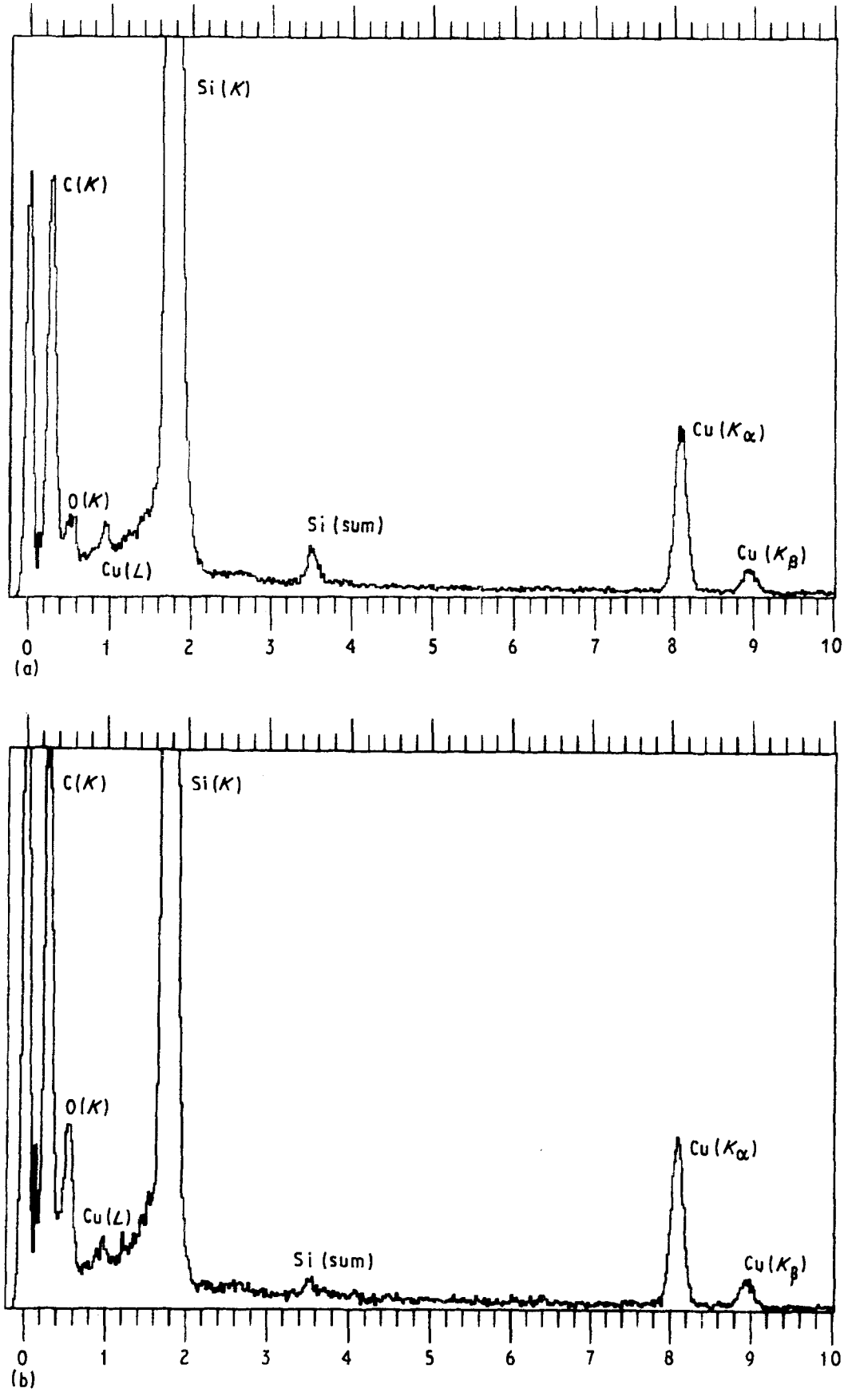

Figure 8 EDX microanalysis of the Isolite whiskers at 20 eV 1 chan and spectrum length = 1024 chan: (a) central region of a whisker at 2 K FS:B and live time = 74 s; (b) near the whisker surface at 1 K FS:B and live time = 100 s; (c) an isolated spherical inclusion at 4 K FS:B and live time = 46 s.

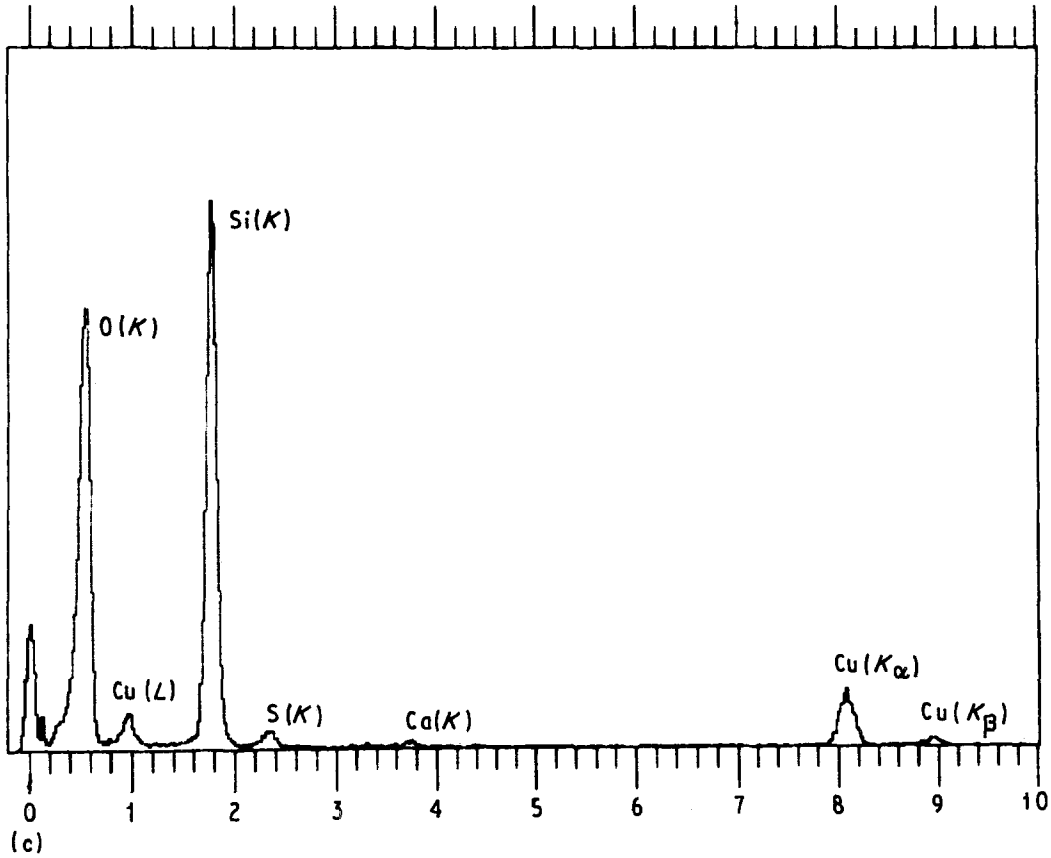

Figure 8 Continued.

whiskers seem to contain much lower impurity levels than have been reported previously in whiskers manufactured by ARCO, Tokai and Tateho [19, 21].

2.2. Tateho whiskers

Two different batches of whiskers were examined dating some years apart (see Table I). Fig. 9 compares the two generations of the Tateho product. They are seen to have approximately the same range of size and aspect ratio but there are clear differences in surface morphology, the earlier whiskers showing a highly irregular and re-entrant surface profile. This difference is clearly shown on studying Figs 9b and d which also show the similar nature of the defect populations in the two generations of whisker. These defects transverse to the whisker axis are believed to be similar to the microtwin defects identified by Nutt in ARCO whiskers [24]. Higher resolution images (Fig. 10) show a very closely, spaced array of defects which introduce considerable one-dimensional disorder into the stacking which is represented by the severe streaking seen on the diffraction pattern. Not all the whiskers showed these defects along their complete length, in Fig. 11 regions which were defect free are shown. In such whiskers the defect-free regions had a much smoother whisker surface profile than was seen where microtwins intersected the surface.

A number of the highly twinned whisker showed gross defects in the form of very large voids in their centres. In some cases (Fig. 12) these voids were seen to run almost the full length of the whiskers. In other whiskers the voids were smaller and accompanied by further volume defects of diameter 5–10 nm (Fig. 13). Similar results were reported by Nutt [19, 24] who also reported voids and inclusions in ARCO whiskers.

EDX microanalysis of the later Tateho whiskers was carried out in a Philips CM12 TEM equipped with thin window detectors. This was not capable of detecting carbon or oxygen signals. In Fig. 14 the predominant peak from the whiskers is seen to be silicon with a large copper signal from the specimen grid. In Fig. 14a, a dense region of an inclusion-containing whisker is analysed. There is a very large calcium signal and a smaller iron signal, both these impurities were found by Karasek *et al.* [21] in their XPS study of Tateho whisker composition. Nutt also found calcium and iron signals in his study of inclusion composition in ARCO SiC whiskers [19]. In Fig. 14b the analysis is taken over one of the large central voids (e.g. Fig. 12). The calcium signal is now absent but a very weak cobalt signal can be distinguished adjacent to the iron peak. No trace of either aluminium or titanium was detected despite their presence in Karasek's analysis; also cobalt was detected despite its absence in his results.

2.3. ARCO whiskers

These are the only whisker samples which were not examined loose. They were supplied in the form of a slab of metal matrix composite, consisting of ~ 20% by volume SiC whiskers incorporated in a 2124 aluminium alloy. This material is very similar to that which has been studied extensively by Nutt [19, 24] and our results confirm much of his work. The composite was

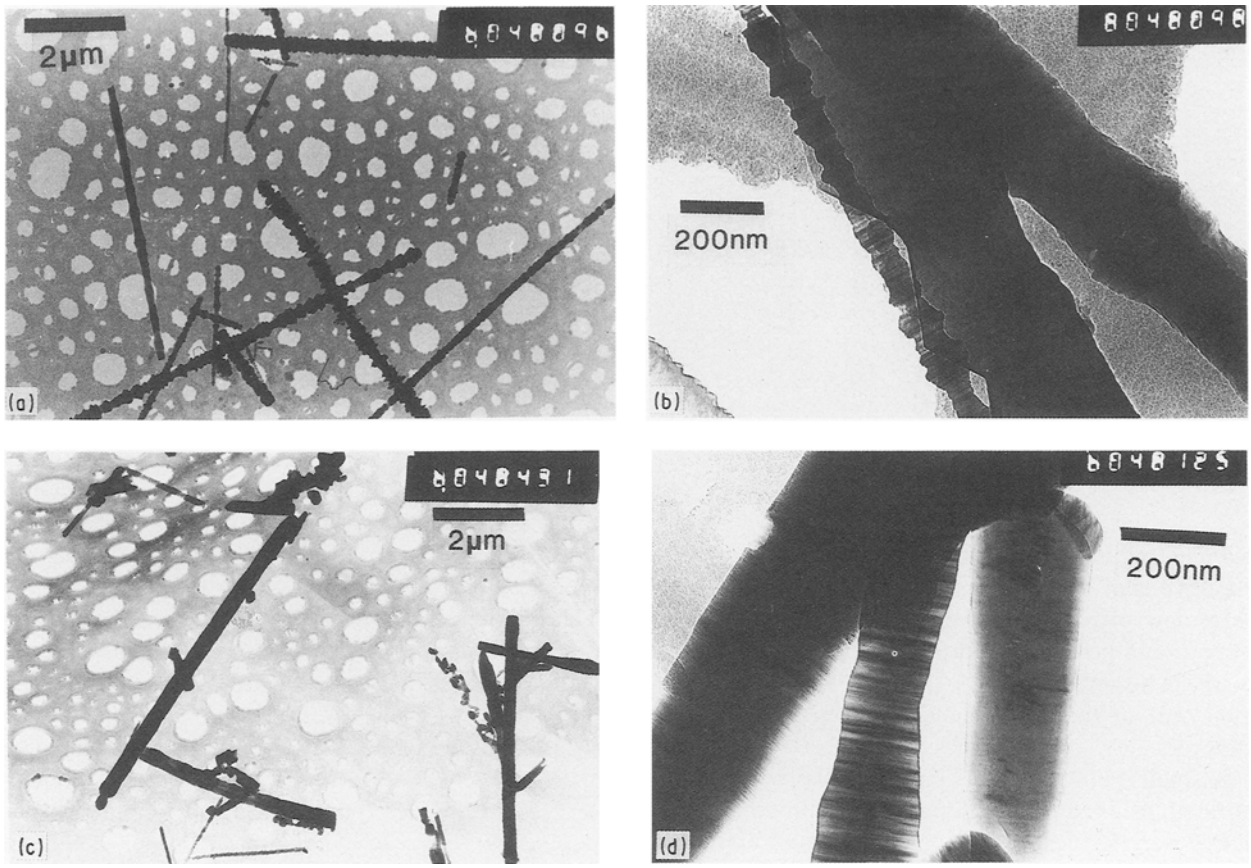

Figure 9 Tateho SiC whiskers. (a) General view of early Tateho whiskers. (b) Early whiskers showing irregular surface profile and transverse defects. (c) Later Tateho whiskers with smoother surface profile. (d) Later Tateho whiskers showing transverse defects and evidence of a core region of different contrast.

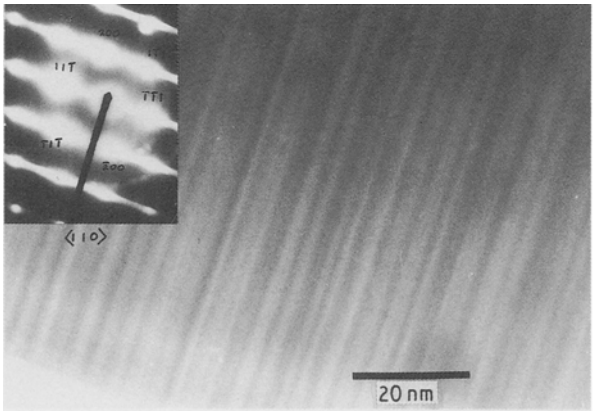

Figure 10 TEM image of parallel twin defects transverse to the Tateho fibre axis. Inset diffraction pattern shows extensive streaking perpendicular to the defects.

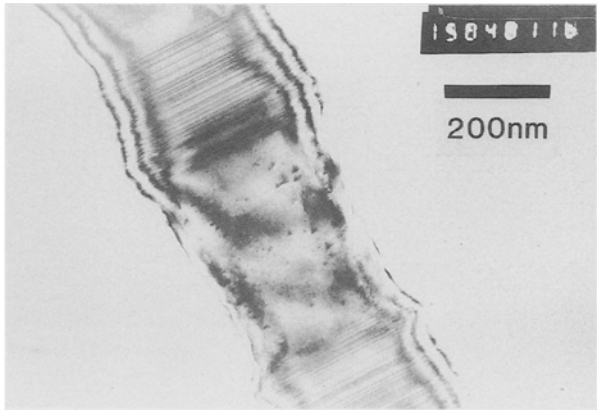

Figure 11 Defect-free region found in some whiskers. These show a smoother surface profile than adjacent twinned regions.

sectioned and thinned to allow images of transverse sections to be viewed. In Fig. 15 one such section is seen alongside a longitudinal view of an ARCO whisker. There is a continuous microtwin distribution as was seen in most of the Tateho whiskers. Transverse sections show a high dislocation density in the (1 1 1) plane around the whisker perimeter but not in the central region of the whisker which shows a mottled contrast. Nutt identified these dislocations with partial dislocation termination of twins near the whisker core. The whisker core was found by Nutt to contain large amounts of impurity inclusion phases such as we found in the Tateho material above.

2.4. Tokai whiskers

The Tokai SiC whiskers appeared similar in some respects to the later Tateho material. Fig. 16 shows transverse defects in a Tokai whisker, similar to those seen in both the Tateho and ARCO whiskers, which on high-resolution imaging are seen to be narrow

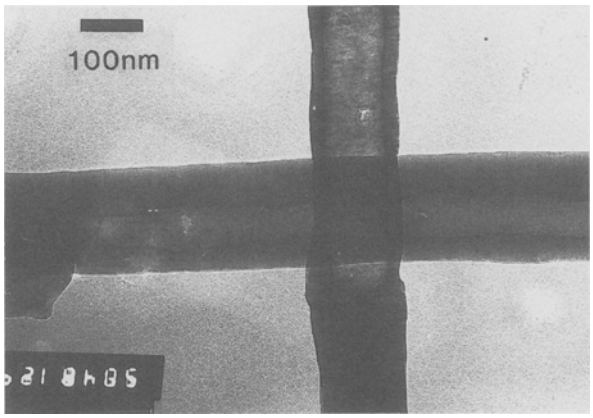

Figure 12 Some Tateho whiskers appear hollow with long void defects running along almost their complete length.

twinned regions. In common with the Tateho material, regions of the whiskers appeared free of the transverse microtwins. However, in the Tokai whiskers these contained further defects inclined at an angle to the whisker axis (Fig. 17) which were slightly reminiscent of the chevron defects seen in the Isolite whiskers.

A small quantity of the Tokai whiskers was incorporated in a commercial purity aluminium matrix. These were fabricated by hot pressing and extrusion. This allowed the preparation of thin transverse sections of the whiskers in the composite such as is shown in Fig. 18. The section is more rounded than the transverse section of the ARCO whiskers in Fig. 15. No dislocations were seen in cross-sections of the Tokai whiskers. However a mottled contrast was seen throughout the section, similar to that seen in the core of the ARCO whiskers.

3. Discussion

There have been a number of papers published in recent years reporting TEM studies of SiC whiskers and platelets. The microtwin defects transverse to the whisker axis have been reported by most workers investigating β-SiC whisker microstructures [15, 17–19, 21, 24, 25]. These defects seem to be common to all methods of whisker manufacture. Chevron defects seen by us in the Isolite whiskers were first reported by Van Torne [26] in whiskers supplied by Thermokinetics. Comer [18] examined whiskers from the same supplier 3 years later and found only the transverse twin defects indicating either a change in manufacturing route or that these defects are very sensitive to manufacturing conditions and their presence or absence varies from batch to batch. Iwanga *et al.* [25] found both types of defect in a single whisker population but each individual whisker contained only one type of defect; however, these whiskers were

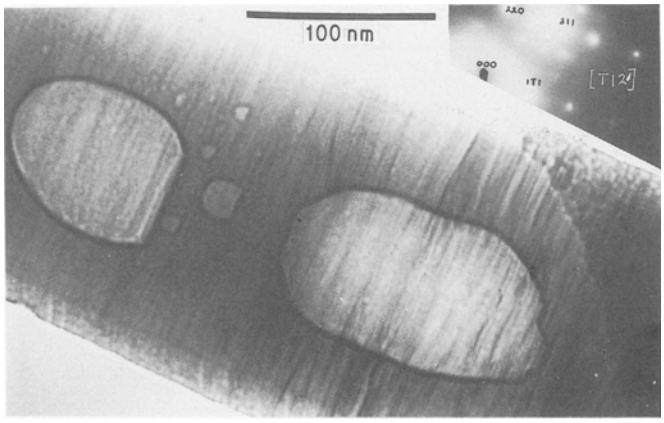

Figure 13 Smaller defects or inclusions seen alongside larger voids in a Tateho whisker.

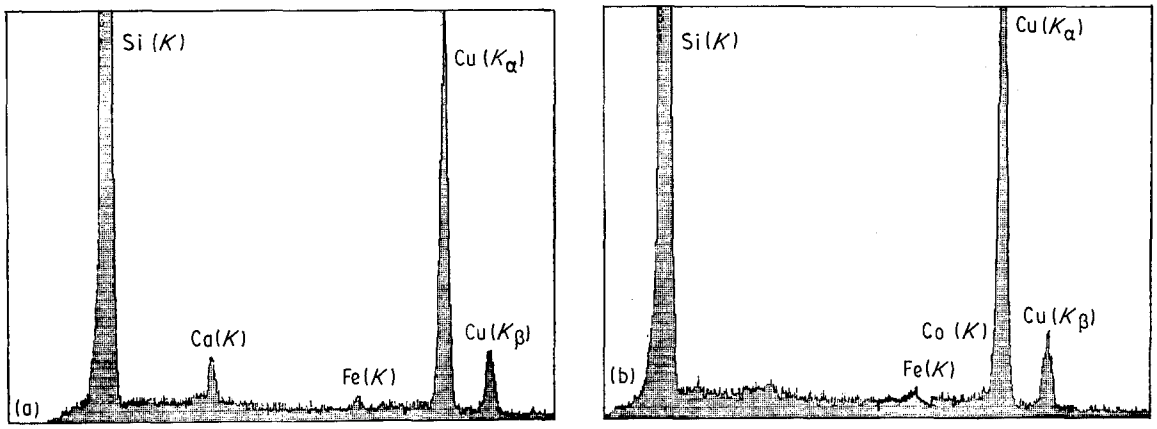

Figure 14 EDX microanalysis of Tateho whiskers showing significant impurity levels of calcium, iron and cobalt. (a) General region of microvoid containing whisker, showing a large calcium peak and a small iron peak. (b) Sampled region over a large central void, no calcium peak but trace iron and cobalt peaks can be identified.

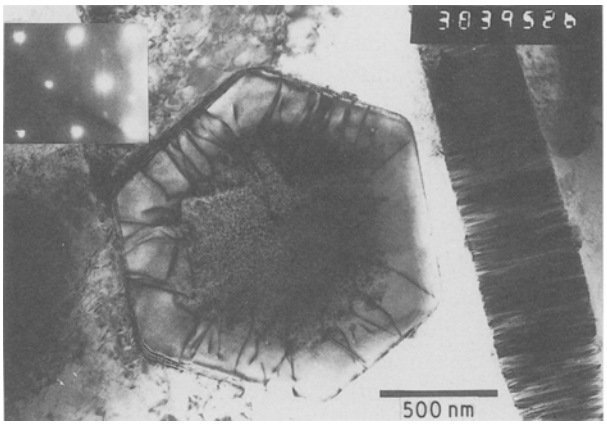

Figure 15 Micrograph of Two ARCO whiskers in a 2124 Al metal matrix composite, one whisker is in a transverse, the other a longitudinal orientation. Core region of the transverse whisker shows mottled contrast ringed by dislocation loops intersecting the surface. The longitudinal whisker shows extensive twinning.

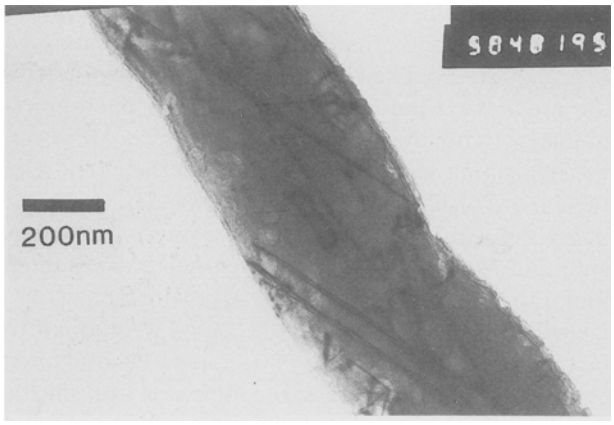

Figure 17 Region on a Tokai whisker free of transverse defects. Other defects of a less distinct nature are visible inclined to the whisker axis.

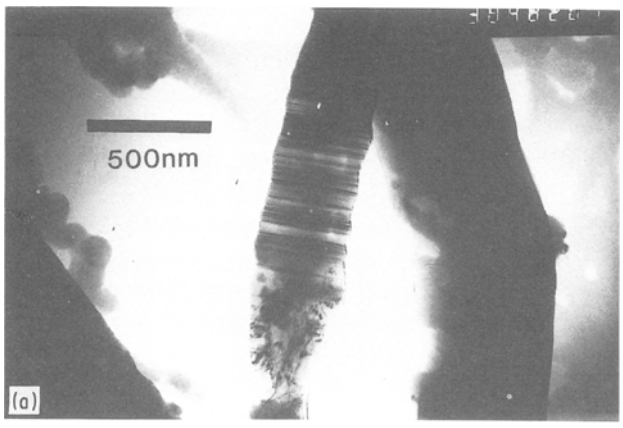

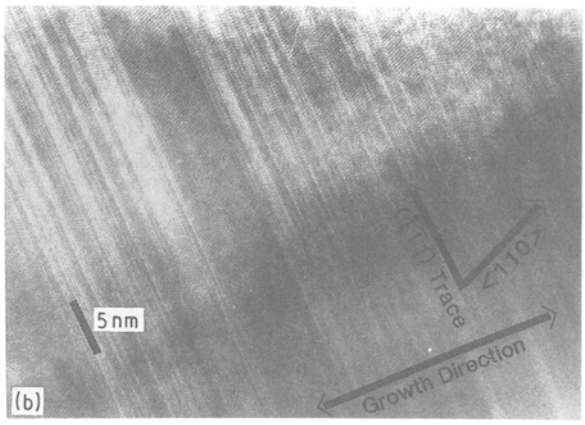

Figure 16 Tokai SiC whiskers. (a) Transmission electron micrograph showing heavily defective whisker region. (b) High-resolution electron microscope image of the parallel defects showing a narrow distribution of twins.

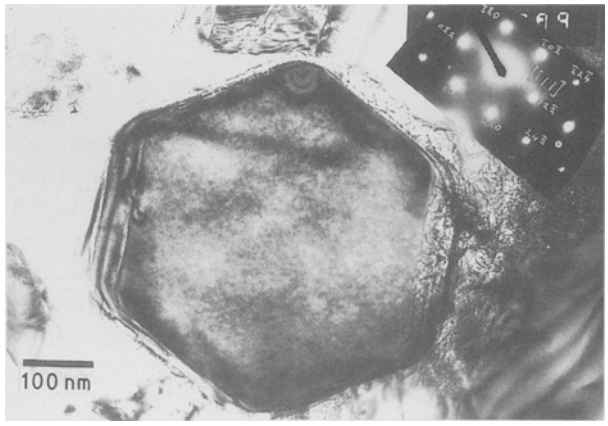

Figure 18 Tokai whisker incorporated into a commercial purity metal matrix composite. Transverse section shows no dislocations although a mottled contrast is seen.

manufactured by a very different route from the other whiskers reported. Iwanga's results are identical to the behaviour of the Isolite material examined in this study. Knippenberg *et al.* [15] reported similar defects to the chevron type but in a SiC platelet. It is possible that one electron micrograph in Knippenberg's work shows both types of defect in the same whisker; however, the contrast difference in the published figure is poor and it is difficult to decide if transverse defects are present.

Whiskers which have the chevron defects tend to have smoother surface profiles than the twinned whiskers. In Fig. 11 the Tateho whisker appears smooth except where the twins occur when a surface roughening is apparent. A similar behaviour is seen in Fig. 16 with the Tokai whiskers and is possibly also occurring in this thin Isolite whisker of Fig. 7c. Thus we can make a tentative hypothesis that twinned whiskers have rougher surface profiles than untwinned ones.

Only one of the whisker types examined (the later Tateho material) showed unequivocal evidence of large void defects along the whisker axis. The presence of such gross defects along the whisker core was also reported by Karasek *et al.* [21] in Tateho whiskers. Nutt [19, 24] reported overlapping microvoids, possibly containing transition metal silicate immunities, along the cores of the ARCO whiskers. A contrast similar to his was seen down the cores of ARCO whiskers in our study (Fig. 15). We also found evidence for small voids or inclusions in our late Tateho whisker samples (Fig. 13).

The presence of gross defects in SiC whiskers was studied some years ago by Bootsma *et al.* [10]. They

investigated whiskers grown by a VLS mechanism during the carbothermal reduction of SiO_2 catalysed by iron particles. The whiskers grown were reported in the range 0.1–1 μm diameter although a micrograph of one >10 μm diameter whisker is shown. However, the interesting feature of this study is their report of regular perturbations in whisker diameter, or knots, along the whisker length. These knots were investigated and from crystallographic symmetry were often found to be associated with a 180° twin on the (1 1 1) growth plane. In their study the knots were found to be contained by {1 1 1} and {1 0 0} side faces and often contained a negative bicrystal comprising iron silicide material. This gave a characteristic core to the knotted regions. There are clearly many similarities here to the observations made on the Tateho, Tokai and ARCO whiskers.

The EDX analyses show the Isolite whiskers to be much purer than the Tateho whiskers and, by inference from the similar chemical analyses reported by Karasek *et al.* [21] for Tateho, Tokai and ARCO whiskers, purer than the other whiskers examined here. In fact, the only trace elements found in the Isolite whiskers appeared in the amorphous SiO_2 phase on the whisker surfaces. The variation in composition found within one Tateho whisker (in particular the calcium peak in Fig. 14) is consistent with Nutt's finding [19] that the impurity phases are concentrated in inclusions, thus the EDX signal recorded will depend on the local number of inclusions in the excited volume. This large difference in the chemical composition between the Isolite whisker and the other whiskers, coupled with their very different defect structure is strong evidence for different whisker growth mechanisms in these two cases.

4. Conclusions

SiC whiskers produced by the carbothermal reduction of SiO_2 are generally believed to form via the combination of the gaseous precursors SiO and CO. It has been shown by Bootsma *et al.* [10] and Milewski *et al.* [11] that the VLS method can be used to catalyse the growth of β-SiC from these precursors. Bootsma was also able to show that the presence of knot defects and inclusions of Fe–Si in the whisker were related to the VLS whisker tip droplet. The precise spacing and nature of the defects were strongly dependent on whisker growth conditions. Nutt [19] postulated a VLS mechanism being responsible for the cored nature of ARCO whiskers. The transverse twin defect structure in the Tateho, Tokai and ARCO whiskers investigated coupled with the evidence of inclusion phases, from EDX, leads us to suppose that these three whiskers grow by essentially the same growth mechanisms; although the local differences in manufacturing practice lead to the different levels of transition metal impurities reported elsewhere for these three whiskers [11, 21]. This mechanism is probably a VLS process with transition metal impurities, or their compounds, acting as the liquid droplets. The use of transition metal compounds as catalysts has, for example, been described in a Tokai Carbon Co. patent for SiC whisker manufacture [23, 27]. This is supported by (i) the incorporation of small inclusion phases, (ii) the highly cored nature of many of the whiskers, and (iii) the high density of microtwins.

The Isolite whiskers are very different in structure and produce defects similar to those reported by Iwanga *et al.* [25] from whiskers fabricated in an oxygen-free environment using silicon metal as the silicon source. Indeed an Isolite patent [14] describes a whisker manufacturing process using reactant gas mixtures of silicon halide and hydrocarbon in hydrogen which is similar in concept to that described in [25]. However, identical defects were seen by Van Torne [26] in whiskers produced using SiO and CO gases. Thus no conclusion can be made as to the cause of these {1 1 1} planar defects on planes not normal to the whisker axis.

We can further conclude that irregular whisker profiles are also associated with the microtwin transverse defects. In all four whisker types surfaces were at least mildly rough in the presence of twins and smooth in the transverse twin-free materials found in the Isolite, Tateho and Tokai samples. The Tateho and ARCO materials contained considerable levels of inclusion and void whisker defects which may in part contribute to the longitudinal splitting failure of whiskers contained in an ARCO whisker-reinforced aluminium alloy metal matrix composite reported earlier [28].

References

1. N. J. PARRATT, in "Verbundwerkstoffe" edited by U. Rösler (DGM, Frankfurt, 1974) p. 253.
2. D. L. McDANELS, *Met. Trans.* **16A** (1985) 1105.
3. S. TOWATA and S. YAMADA, *Trans. Jpn Inst. Met.* **27** (1986) 709.
4. G. C. WEI and P. F. BECHER, *Bull. Amer. Ceram. Soc.* **64** (1985) 298.
5. F. C. FRANK, *Proc. Faraday Soc.* **5** (1949) 48.
6. W. BURTON, N. CABERA and F. C. FRANK, *Phil. Trans. Roy. Soc. Lond.* **A243** (1951) 299.
7. J. B. NEWKIRK and G. W. SEARS, *Acta Metall.* **3** (1955) 110.
8. W. W. WEBB, in "Growth and Perfection of Crystals", edited by R. H. Doremus *et al.* (Wiley, New York, 1958) p. 230.
9. R. W. WAGNER and W. C. ELLIS, *Trans. AIME* **233** (1965) 1053.
10. G. A. BOOTSMA, W. F. KNIPPENBERG and G. VERSPUI, *J. Crystal Growth* **11** (1971) 297.
11. J. V. MILEWSKI, F. D. GAC, J. J. PETROVIC and S. R. SKAGGS, *J. Mater. Sci.* **20** (1985) 1160.
12. E. I. GIVARGIZOV, *Curr. Topics Mater. Sci.* **1** (1978) 79.
13. Tateho Kagaku KK, UK Pat. 2168333A (1986).
14. Isolite Kogyo KK, Jap. Pat. 57-123813A (1984).
15. W. F. KNIPPENBERG, H. B. HAANSTRA and J. R. M. DEKKERS, *Philips Tech. Rev.* **6** (1962/3) 181.
16. J-G. LEE and I. B. CUTLER, *Bull. Amer. Ceram. Soc.* **54** (1975) 195.
17. N. K. SHARMA, W. S. WILLIAMS and A. ZANGVIL, *J. Amer. Ceram. Soc.* **67** (1984) 715.
18. J. J. COMER, *Mater. Res. Bull.* **4** (1969) 279.
19. S. R. NUTT, *J. Amer. Ceram. Soc.* **71** (1988) 149.
20. K. M. MERZ, in "Silicon Carbide, A High Temperature Semiconductor", edited by R. J. O'Connor and J. Smiltens (Pergamon, Oxford, 1960) p. 73.
21. H. R. KARASEK, S. A. BRADLEY, J. T. DONNER, M. R. MARTIN, K. L. HAYNES and H. C. YEH, *J. Mater. Sci.* **24** (1989) 1617.

22. M. F. STANTON and M. LAYARD, "The Carcinogenicity of Fibrous Minerals", NBS special Pub. 506 (National Bureau of Standards, Washington, DC, 1978) p. 143.
23. Tokai Carbon KK, Jap. Pat. 62-113 800A (1987).
24. S. R. NUTT, *J. Amer. Ceram. Soc.* **67** (1984) 428.
25. H. IWANGA, T. YOSHIIE, H. KATUKI, M. EGASHIRA and S. TAKEUCHI, *J. Mater. Sci. Lett.* **5** (1986) 946.
26. L. I. Van TORNE, *J. Appl. Phys.* **37** (1966) 1849.
27. Tokai Carbon KK, UK Pat. 2116 533A (1983).
28. S. M. PICKARD, B. DERBY, J. HARDING and M. TAYA, *Scripta Metall.* **22** (1988) 601.

Received 12 October 1990
and accepted 20 March 1991